Moisture evolution, thermal properties and energy consumption of drying spent grain pellets from a blend of some cereals for small scale bio-energy utilization: Modelling and Experimental study.

NdukwuM.C[a*]; Horsfall I.T[a]; Lamrani B[b]; Wu H[c]; Bennamoun L[d]

[a]Department of Agricultural and Bio-resources Engineering, Michael Okpara University of Agriculture, Umudike, P.M.B. 7267 Umuahia, Abia State, Nigeria.

[b] Mohammed V University in Rabat, Faculty of Sciences, MANAPSE Laboratory, Rabat, Morocco.

[c]School of Engineering and Computer Science, University of Hertfordshire Hatfield, UK
[d]Department of Mechanical Engineering, University of New Brunswick, Fredericton, Canada

*Email:ndukwumcu@mouau.edu.ng, Phone: +2348032132924

Abstract

A fixed bed convective dryer was used to assess the influence of drying temperature and geometry deformation on moisture and thermo-physical property evolution of solid fraction pellets (spent grain) from wet milling of cereal blends for bio-energy generation for small homes. The aim is to study the physical mechanism of drying the pellets that includes temperature and moisture behaviour, transport phenomena, the response rate to varying process conditions, drying time, and energy utilization which can be applied in the development of a fixed bed dryer for drying the pellets at a lower scale. The Modified Cranck's diffusion model was used to study moisture loss by introducing shrinkage. The verification of the model gave the mean absolute error (MAE) for moisture content with shrinkage as 0.0366 - 0.1500 while for without shrinkage was 0.0729 - 0.1500 for 60- 80 °C. The effective moisture diffusivity with integrating shrinkage is lower than non- shrinkage though these values varied with drying time. Fitting the moisture ratio with the exponential drying curve equations shows that logarithmic equations were the best model for drying at 60 and 70 °C while Henderson and Pabis's model was better at 80 °C isothermal drying. Thermo-physical analysis showed that the average specific heat capacity ranges from 5423.387 to 5198.197J/kgK while the thermal conductivity ranged from 0.115281to 0.136882W/mK at 60-80 °C. The energy and specific energy consumption ranged from 0.41 to 0.494 kWh and 108.39 to 119.29MJ/kg. The shrinkage ratios, effective diffusivity and energy and specific energy consumption were empirically presented as a function of moisture, temperature and or air velocity variations with a high degree of association.

Keywords: Pap production; cereal processing; heat and mass transfer; drying; thermal analysis

Nomenclature

D	Diffusivity (m^2/s)	Greek letters	
Dv	Mass diffusion of air-water vapour (m^2/s)	ε	porosity
n	Number of product on the tray	ρ	Density (kg/ m^{-3}),
t	Time (h)	ν	Kinematic viscosity (m^2/s).
M	Moisture constituent (kg/kg or %)	α	Thermal diffusivity of air (m^2/s)
m	mass(kg)	μ	Dynamic viscosity (Pa.s)
C_p	The specific heat capacity (J/kg K)		
L	Thickness (m) or length (m)	Subscript	

P	Pressure (bar)	o or i	Initial
T	Temperature (^{o}c)	a	air
k	Thermal conductivity (W/mk)	ref	Reference
h_c	Convective heat transfer coefficient (W/m^2 K),	e	Equilibrium
A	The surface area of the dried product (m^2),	eff	effective
Nu	Nusselt number.	p	product
p	The perimeter of the sample (m).	atm	Atmospheric
dh	Hydraulic diameter (m) and		
Re	Reynolds number		
Xv	Molar fraction of water vapour		
v	The velocity of drying air (m/s)		
w	Weight (kg)		
V	Volume (m^3)		
MR	Moisture ratio.		

1. Introduction

Pap or cereal pudding (Ogi or Akamu) is a starchy slurry that is a product of wet milling of cereals that includes maize or millet with the addition of sorghum or blending any of the two or all the mentioned cereals. Pap serves as a weaning food for infants or breakfasts for adults in most countries [1]. During the production process, after washing, mixing, steeping, fermenting, and milling the grain, they are centrifuged to separate the starch slurry from the solids fraction (spent grain) made up of the bran, hulls, and germ. The solid fraction with different levels of soluble is either further processed or thrown away. However, they are rich in probiotics; prominent among them is Lactic acid bacteria (LAB) regarded as nutritional supplements having a potential benefit for centuries as natural constituents in health-promoting foods for man and animals [2]. Therefore, the wet solid fractions can form part of the animal feed ration for cattle, chickens, and goats if neatly collected. The major concern is its short shelf –life. Most by-products of fermented wet grains cannot be stored in wet conditions for more than four days in warm weather conditions and seven days at 10 ^{o}C [3]. This is because, besides the LAB produced during fermentation, they can also harbour different kinds of fungi that produce mycotoxins if stored under warm conditions. These mycotoxins; namely fumonisin, aflatoxin, and zearalenone can be toxic and carcinogenic at higher levels of occurrence, and therefore become not suitable as feed ingredients [4]. The United States Food and Drug Administration FDA [5] has put in place regulations for the acceptable level of mycotoxins in grains for consumption [6,7]. Contaminated grains used in livestock feed reduce their productivity and adversely affect their health. Therefore, they are more suitable as biomass for bio-energy generation even at a small scale of individual home utilization.

Tons of mixture of maize, sorghum and millet spent grain from pap production are produced across West Africa every day at both subsistent and commercial levels though the actual value is yet to be quantified. However, management of this spent grain poses a challenge to the pap processors because of having no means of processing, preserving and storing them. Therefore, they discard them as waste in most cases. One of the ways to increase the shelf- life of spent grain and make it more available is by drying. Drying reduces the moisture content to a safe storage level required for its valorisation as bio-fuel. Therefore in this research, pellets formed from the mixture of maize, sorghum and millet processing were thermally dried in a box-type fixed bed dryer. The drying behaviour was investigated within the range of control factors that includes drying temperature, the geometry of dried solid waste and drying air velocity. Additionally, thermal properties and energy consumption analysis were studied at different temperatures and drying times. This has become imperative because every solid waste has its unique characteristics and consequently has its unique thermo-physical properties different from others based on the parent material they are derived from and how it was processed.

Several studies on the drying of spent grain abound in literature [8-11] but none has been studied on the spent grain pellets from the mixture of maize, sorghum or millet processing as done in pap production or cereal pudding. Most of the studies focus on large spent grain from breweries usually dried with rotary drum driers. This has alienated the small scale cereal processors, whose waste generated might not be cost-effective to deploy rotary drum driers. In most developing countries women with lower income are the dominant cereal processors at small scale levels and cannot afford commercial rotary drum driers. Those who tried to process the spent grain for future use always form them into handmade pellets and dry them under the sun for long days due to the initial high moisture content and starch granules present. This makes the whole process very tedious as the women have to divide their time into going to the market to sell the slurry produced, going to the farm to harvest the cereals, and battling with the weather to avoid rewetting the drying spent grain and also other intruders. Therefore, they prefer throwing this away which is the major reason this waste can be seen littered at different dump sites across developing countries like Nigeria. However, the provision of small low-cost fixed bed dryers within homes can help valorise this waste at a lower scale and turn them into useful products for energy generation for homes. To do this, first, the physical mechanism of drying them that includes temperature and moisture distributions, transport phenomena, the response rate to varying process conditions, drying time, and energy consumption must be studied. Physical interpretation of this drying mechanism needs to be presented to aid in the understanding of the optimum parameters (velocity, porosity, bulk and particle density, sorption-desorption behaviour, permeability, thermo-physical properties, temperature and relative humidity) that can be applied in the designing of the fixed bed dryers [12]. Therefore, for this aspect, this research is justified. The objective of this research, therefore, is as follows (1) provision of literature on drying characteristics of solid fraction from wet milling of a mixture of cereal pellets from maize, sorghum and millet as done locally in most countries that produce pap (2) drying kinetics, thermo-physical properties and energy consumption analysis (3) Empirical presentation of the effect of moisture variation and temperature on shrinkage, moisture diffusivity and energy consumption of solid fraction from wet milling of grains.

2. Materials and methods

2.1 Materials

Maize, sorghum and millet were obtained from an open market in Umuahia South Eastern Nigeria. The various grains were sieved of chaffs and other impurities before blending (2:1:1 ratio for maize, sorghum and millet respectively) and washing thoroughly. The blend was soaked in clean water for three days to allow for adequate fermentation before wet milling with an attrition mill. The milled cereals were sieved with a silk cloth and further centrifuged to separate the starch slurry (pap) from the solid fractions (spent grain) as done locally by producers. However, as it has been noted during the sieving process, some soluble starch remains with the wet solid waste. The spent grain was formed into cuboid-shaped pellets (length given as X = 0.067 m, width Y= 0.048 m and thickness Z = 0.018m) with the soluble starch acting as the binder. Pelleting was manually done by forcing a compacted wet spent grain through a horizontal steel hole (X = 0.067 m, width Y= 0.048 m and thickness Z = 0.018m). The initial moisture contents of the pellets were determined by drying three sets of 43.0 ±0.08A g pellets in a laboratory oven ((DHG-9053A Ocean med+ England) at a constant temperature of 105 °C for 24 h. The initial moisture content determined was 0.65 kg/kg (w.b). The mass of the pellets was determined with a digital weighing balance (Scout Pro SPU 405, China) with an accuracy of 0.01 g. The dimensions of the pellets were determined with venire calliper (Mitutoyo, JIS.B.7502.). The fixed bed dryer (Fig 1) consists of a box-type oven drying chamber with the heating element (2000W) mounted at the top above the drying trays. The suction fan was mounted on the back wall opposite the door. The thermostat regulates the temperature of the dryer. The walls were insulated with fibreglass to prevent heat loss.

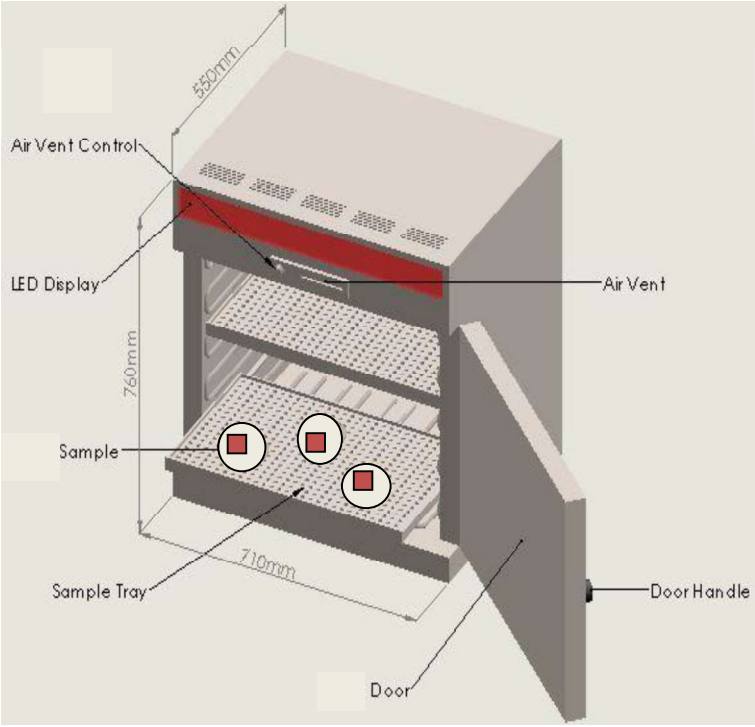

Fig. 1. Schematics of the box-type oven drying chamber experimental setup

2.2 Experimental procedure

The drying runs were undertaken with a box-type convective fixed bed dryer. Three sets of pellets of equal dimensions were placed on a drying tray (0.04155 m^2) inside the dryer and dried for each run. A load cell measures the weight loss while the airspeed was kept constant at 0.8 m/s. Drying was done at three constant drying temperatures of 60, 70 and 80 ^oC respectively. The room temperature during the experiment ranges from 28.2 to 29.1 ^oC. The temperature and humidity were measured with a K- type thermocouple linked to Omega type data logger ((HH1147; Omega, Stanford, USA). Twenty-seven samples were dried for the entire duration of the experiment until they reach constant weight under the drying conditions.

2.4 Mathematical modelling

To introduce shrinkage into the moisture content determination, Bennamoun et al [13] have shown that the solution of the Crank diffusion model by Efremov and Kudra [14] presented in equation 24 using the Fourier number (Fo) gave a better prediction of moisture content behaviour during drying of bio-products. According to Efremov and Kudra [14], placing n=1 in equation 1 gives an error of 3 9%. Therefore they gave the analytical model presented in equation 2, using the Fourier number for plates and spheres and introduced a correction factor for shrinkage to evaluate the moisture content. The correction factor was determined by taking the minimum deviation from the exact solution of the crank solution in equation 1. This model has been tested with different products with a good result

$$\frac{m_t - m_e}{m_o - m_e} = \frac{6}{\pi^2}\sum_{n=1}^{\infty}\frac{1}{n^2}\exp(-\pi^2.n^2.Fo) \quad (1)$$

$$\frac{m_t - m_e}{m_o - m_e} = \exp(-\pi^2.Fo^a) \quad (2)$$

To calculate the equilibrium moisture content (m_e), the modified Oswin equation [15] was used to describe the sorption isotherms (m_e) of the spent grain pellet as follows

$$m_e = [A + B(T - 273.15)]\left[\frac{RH}{1-RH}\right]^{1/C} \quad (3)$$

Where A, B and C are the empirical parameters given as 0.19299, 0.0019449 and 1.517 respectively for desorption while for adsorption it is given as – 0.15234, -0.001643 and 1.639 [15] respectively, RH is the relative humidity.

$$Fo = \frac{D_{eff}.t}{L^2} \quad (4)$$

L is the characteristic length, a is a correction factor given as 0.91 for a plane surface. The effective moisture diffusivity is deduced as follows

$$D_{eff} = \frac{L.h_m}{Bi} \quad (5)$$

The mass transfer coefficient (h_m) therefore, was deduced by combining it with the heat transfer coefficient [16] as follows

$$h_m = \frac{h_c}{\rho_a C_{pa} (Le)^{1/3}} \quad (6)$$

Where, c_{pa} is the specific heat of air (J/kg ^oC) determined from Merlin et al et al. [17] as follows:

$$C_a = 1161.482 - 2.368849T + 0.01485511T^2 - 5.034909x10^{-5}T^3 + 9.928569x10^{-8}T^4 - 1.111097x10^{-10}T^5 + 6.540196x10^{-14}T^6 - 1.573588x10^{-17}T^7 \quad (7)$$

ρ_a (kg/m^3) is the density of humid air given as follows [13]

$$\rho_a = (3.484 - 1.317X_v)\frac{atm}{273.15} \quad (8)$$

$$Le = \frac{\alpha_a}{D_V} \quad (9)$$

Where α_a (m^2/s) is the thermal diffusivity of air given as 2.18 x10^{-5} m/s^2, while D_v is the mass diffusivity coefficient of air-water vapour

$$D_v = \frac{2.25x10^{-5}}{P_{atm}}\left(\frac{T_a}{273}\right)^{1.81} \quad (10)$$

The convection heat transfer coefficient (h_c) and other thermal properties of air was calculated from the equations suggested in the works of Vaibhav et al. [18] , Merlin et al [17] and Merlin and Ndukwu [19] as follows :

$$h_c = Nu \times \frac{k_a}{dh} \quad (11)$$

Thermal conductivity of air is deduced from as follows

$$k_a = 7.57x10^{-5}T_a + 0.0242 \quad (12)$$

However, the hydraulic diameter can be determined from equation [18] as:

$$dh = 4 \times \frac{A}{P} \quad (13)$$

$$Nu = 0.615 \times (Re)^{0.456} \quad (14)$$

The Reynolds number is deduced with the hydraulic diameter as follows

$$Re = u \times \frac{dh}{\nu} \quad (15)$$

$$\nu = \frac{\mu_a}{\rho_a} \quad (16)$$

$$\mu_a = 1.718x10^{-5} + 4.620x10^{-8}T_a \quad (17)$$

The biot number (Bi) is calculated as follows

$$Bi = \frac{R_e h_m}{Dv} \quad (18)$$

Statistical evaluation

The obtained results were verified using the mean absolute error (MAE), and the standard error (SE) as reported by Simo-Tagne et al. [20] as follows.

$$MAE = \frac{1}{N}\sum_{i=1}^{N}\left|m_{exp,i} - m_{pred,i}\right| \quad (19)$$

$$SE = \frac{\sqrt{\sum_{i=1}^{N}\left(m_{exp,i} - m_{pred,i}\right)^2}}{N-1} \quad (20)$$

2.3 Experimental Shrinkage and moisture content

The shrinkage of the pellets was determined in terms of volume reduction. The length, breadth and thickness of the pellets were manually measured at one-hour intervals using a veneer calliper and the volume was determined as a volume of a cuboid. The shrinkage of the pellets was deduced as follows

$$1 - \frac{V_t}{V_0} \quad (21)$$

The experimental moisture content during the drying process at a different time interval (t) was determined with Equation 22 as presented in Das Purkayasthaet al [21] as follows

$$m_t = \left[\left(\frac{W_t}{W_i}\right)\{(m_i + 1) - 1\}\right] \quad (22)$$

2.4 Effective moisture diffusivity of the pellets

The solution of equation 2 by Efremov and Kudra [14] gave shrinkage effective diffusivity as

$$D = \frac{L^2}{\pi^{2/a_t}}\left(-\ln(MR)\right)^{1/a} \quad (23)$$

However, Kumer et al [22] also gave an empirical equation for temperature-dependent effective diffusivity as follows

$$\frac{D_{ref}}{D_{eff}} = \left(\frac{V_0}{V}\right)^2 \quad (24)$$

2.5 Drying kinetics

The experimental moisture ratios were fitted into three exponential drying curves presented in Table 1. The simulated moisture ratio results obtained from the curves were compared with the experimental data at temperature ranges of 60, 70 and 80 ºC. The measured moisture contents of the product were compared to the simulated results. Statistical comparison was made and analysing of the coefficient of determination (R^2) followed by the root mean square error (RMSE) values for the best fit model to predict the drying curves of the pellets

Table 1: Model equations for drying curves

Model name	Model	Reference
Newton/Lewis	$MR = e^{-kt}$	[23]
Henderson and Pabis's	$MR = ae^{-kt}$	[23]
Logarithmic model	$MR = ae^{-kt} + c$	[23]

2.7 Thermal properties

2.7.1 Specific heat and thermal conductivity

The dominant cereal, in the spent grain, is mainly maize (50 %) millet (25%) and sorghum (25%). Therefore the specific heat capacity (J/kg K) was determined with the equations 25, 26 and 27 for temperatures of 60, 70 and 80 ^oC respectively as presented by Ariku et al [23] for the variation of moisture content (% w.b) with the specific heat capacity of cereals at a temperature range of 50 - 80^oC as follows

$$C_p = 109.6M + 1116 \quad (25)$$

$$C_p = 143.9M + 711.4 \quad (26)$$

$$C_p = 136.6M + 923 \quad (27)$$

The thermal conductivity is given by Dutta et al. [45] for bulk cereals as follows

$$k = -0.5 + 0.00255T - 0.00000213T^2 + 0.00424M - 0.00000656M^2 + 0.00000648MT \quad (28)$$

2.8. Energy consumption for drying

The total amount of energy consumed in drying the pellets is given by Motevail et al [24] as follows

$$E_c = E_{bd} + E_{bl} \quad (29)$$

Where E_{bd} is the energy consumed (kWh) in moisture removal from the pellet, E_{bl} is the energy utilized by the fan

$$E_{bd} = Au\rho_a C_{pa} D_T t \quad (30)$$

A is the total area of the drying tray given as 0.04155 m^2, D_T is the drying temperature difference (^oC), u is the air velocity fixed at 0.8m/s, C_{pa} is the specific heat of the air taken as 1.00504kJ/kg ^oC, ρ_a is the density of air taken as 1.073kg/m^3, and t is the total drying time (s).

$$E_{bl} = = \frac{u^2 t}{16600} \quad (31)$$

The specific energy consumed (kWh/kg) is given by Ihediwa et al [25] as

$$E_{sp} = \frac{E_c}{W_o} \quad (32)$$

Where w is the amount of water removed from the samples given as:

$$w_o = w_t - w_{t+1} \quad (33)$$

Where, W_t is the weight (kg) at time t (hr) and $W_{t+1}$is the next weight (kg) after W_t

2.9. Uncertainty error Analysis

The uncertainties or statistic limit error of measurement of length, width, thickness and mass of the product was determined using the bias uncertainty error synthesis as presented by Baniasadi et al [26]. The precision error from

sets of measured data (Z)was determined using their standard deviation of the measured data in triplicate. The statistical bias uncertainty error (B_u), standard deviation and the overall uncertainty is presented with equation 34-36 respectively as follows

$$B_u = \frac{\sigma}{\sqrt{n}} \quad 34$$

$$\sigma = \sqrt{\frac{1}{(n-1)}\sum(Z_i - \bar{Z})^2} \quad 35$$

$$\frac{U_o}{S} = \sqrt{\left(\frac{B_u}{K}\right)^2 + \left(\frac{P_u}{K}\right)^2} \quad 36$$

Where Pu is the total possible errors from the measurement using the instrument and taken from the precision of 0.001, n is the number of parameters, and K is the measured parameter. The results of the obtained error for the measurements using the digital instruments are shown in Table 2. The overall uncertainty for the measurements ranges from 1.56 % to 7.08 %.

Table 2: Statistical limit error (Uncertainty)

Temperature	measured	1st data	2nd data	3rd data	$\bar{Z}$	Σ	B_u	Uo/s
60 ° C	L (m)	0.0653	0.0661	0.065362	0.0656	0.00048	0.00046	0.0158
	W(m)	0.0481	0.0471	0.0475	0.0476	0.00114	0.00066	0.0252
	T (m)	0.0147	0.0175	0.0144	0.0155	0.00126	0.00073	0.0702
	M (kg)	0.0308	0.0283	0.0293	0.0295	0.00116	0.00067	0.0409
	L (m)	0.0649	0.0649	0.0648	0.06488	0.0003	0.00018	0.0156
	W(m)	0.0474	0.0462	0.0474	0.04701	0.0006	0.00034	0.02246
	T (m)	0.0146	0.0146	0.0144	0.01451	0.0002	0.0001	0.0692
70 °C	M (kg)	0.0309	0.0305	0.0297	0.03033	0.0010	0.00059	0.0383
	L (m)	0.0638	0.0634	0.0638	0.0637	0.0002	0.00013	0.0158
80 °C	W(m)	0.0451	0.0454	0.0452	0.0452	0.0001	0.00007	0.0222
	T (m)	0.0132	0.0122	0.0127	0.0127	0.0005	0.00028	0.0708
	M (kg)	0.0295	0.0294	0.0291	0.0293	0.0002	0.0001	0.0343

3. Results and Discussion

3.1 Moisture and shrinkage evolution of the pellets

Moisture transport in materials like porous spent grain pellets is driven by a complex mechanism that accounts for the phase motion [27]. This motion of moisture is a function of the thermal environment, material porosity, available pores and the conditions of these pores [28]. For a continuous porous material, the heat flux gradient can be carried by the moisture flux [27]. Therefore, due to temperature increase, moisture is transported to the surface for mass transfer to occur (moisture loss). Figure 2 shows the drying rate (moisture loss rate) of the isothermal drying of the pressed spent grain cake. At first 0.5h of drying, the drying rates were 0.120, 0.133 and 0.151 kg of water/kg of dry solid. hr for 60, 70 and 80 °C but decreased with time respectively. Though the drying rate follows falling rate characteristics like most biological materials it wasn't a smooth curve as has been observed by drying similar materials like olive waste pulp [29]. This is due to the presence of more than one diffusion period that is common to

thermoplastic and hygroscopic materials, resulting in case hardening that prevents capillary movement of moisture to the surface [30]. This kind of case is more common in fruits that have low melting sugar [31].

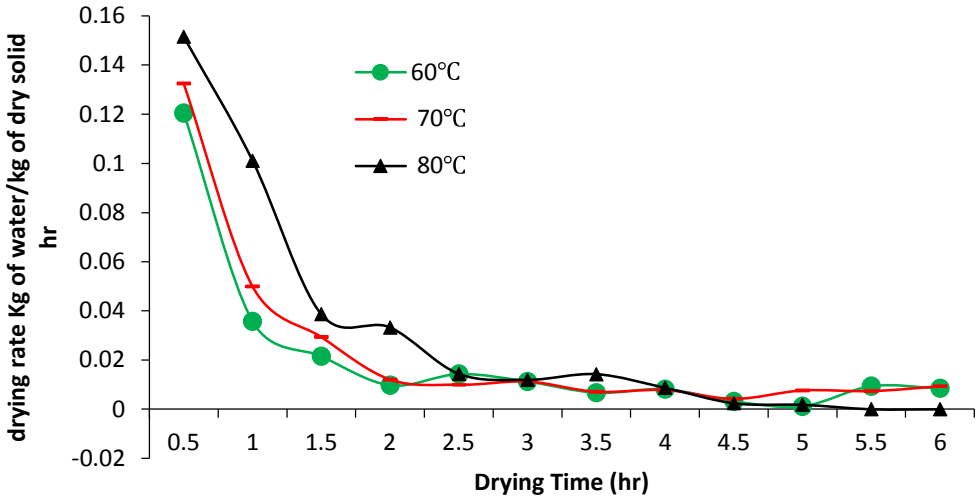

Fig.2. the drying rate of the pellets

Figure 2 showed the calculated shrinkage and moisture content curves of the pellets after 6 hours of continuous drying at different temperatures. Shrinkage was considered in lengths, width and thickness embodied in the volume change from the initial volume. From Figure 3, the degree of shrinkage increased as the drying time progresses due to pore water depletion from the pore capillaries of the pellets. Shrinkage was a result of the collapse of the internal structure of the pellets. In the beginning, the degree of shrinkage was higher for 80 °C due to rapid moisture loss but after 3 hrs 70 °C showed higher shrinkage. Generally drying at 60 °C showed lower shrinkage all through the drying period. The volume shrinkage was correlated to the moisture ratio using a non-fit Hyperbolic Decline non-linear regression equation. The model equations are presented in equations 35, 36 and 37 for 60, 70 and 80 °C isothermal drying respectively with R^2 ranging from 86 to 97 %. The high R^2 values obtained showed that equations 37 – 38 can predict the volume shrinkage at the respective temperatures

$$V_{60} = 0.89V_o\left(1 - \left({}^{9.7MR}/_{15.17}\right)\right)^{({}^{-1}/_{9.7})} \quad R^2 = 0.86 \quad 37$$

$$V_{70} = 0.82V_o\left(1 - \left({}^{3.64MR}/_{6.96}\right)\right)^{({}^{-1}/_{3.64})} \quad R^2 = 0.92 \quad 38$$

$$V_{80} = 0.90V_o\left(1 - \left({}^{21.5MR}/_{24.3}\right)\right)^{({}^{-1}/_{21.5})} \quad R^2 = 0.97 \quad 39$$

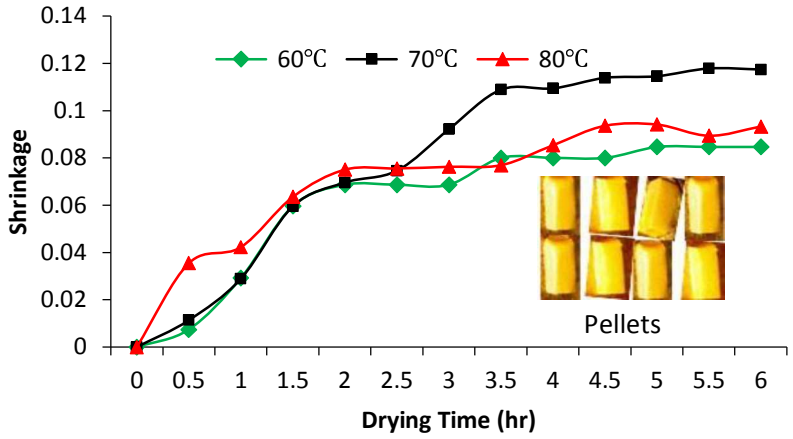

Fig. 3. Shrinkage curve for the drying process

3.2 Evolution of moisture content with and without shrinkage

The deformed geometry model of equation 2 was used to introduce shrinkage into the moisture gradient variation with and without shrinkage as presented in Figure 4 (a-c) for different temperatures and drying times. The veracity of the predicted moisture content was verified using mean absolute error (MAE), and standard error (SE). The obtained values of MAE for moisture content with shrinkage were 0.0366, 0.0786 and 0.1500 for 60, 70 and 80 ºC respectively while without shrinkage it was 0.0729, 0.1033 and 0.1506 for 60, 70 and 80 ºC respectively. The standard error values with shrinkage were 0.0191, 0.0311 and 0.0521 for 60, 70 and 80 ºC respectively while without shrinkage it was 0.0267, 0.0359 and 0.0432 for 60, 70 and 80 ºC respectively. The MAE and SE values for modelling with the integration of shrinkage for all temperatures were lower when compared with modelling without integration of shrinkage. Therefore, modelling with the integration of shrinkage better predicted the moisture content curve values. The relative error showed that integrating shrinkage under predicted the moisture values by just 9.09 % while it was 18.07 % for without shrinkage at 60 ºC, while it was 19.83 % and 25.94 % for 70 ºC and 15.20 and 13.20 % for 80 ºC respectively. From Figure 3 the initial values of the experimental data were higher than the predicted values but seem to converge as the drying progresses with the same trend.

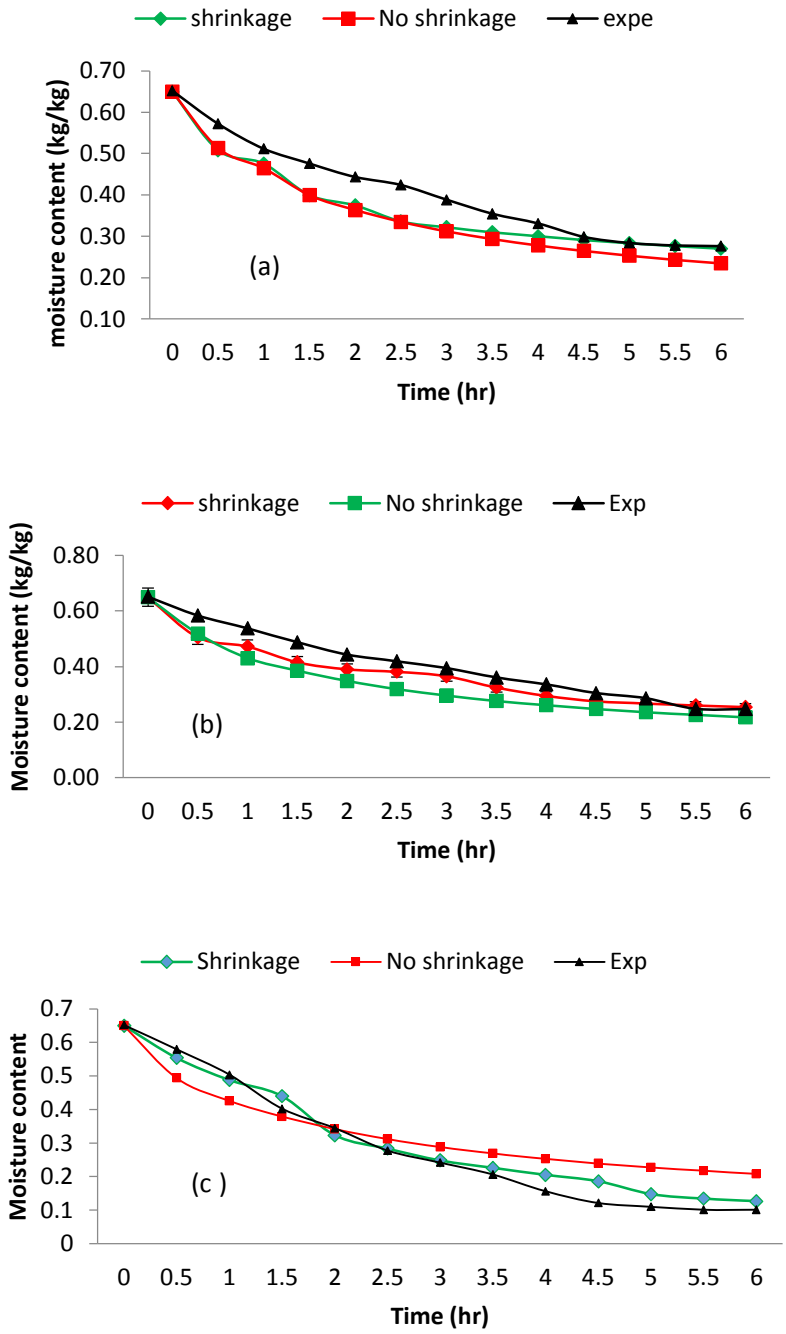

Fig. 4. Predicted and experimental (Exp) moisture Content curve (a) 60°C (b) 70°C (c) 80°C

Figure 5 presents the comparison of the predicted and simulated moisture gradient with experimental values. The R^2 values between the predicted and the experimental values were 0.96, 0.98and 0.99 for 60, 70 and 80 °C respectively for shrinkage while it was 0.94, 0.98 and 0.94 for non-shrinkage at the same temperatures, respectively. These high values showed that the model can be used to explain the moisture behaviour of the pellets under isothermal conditions.

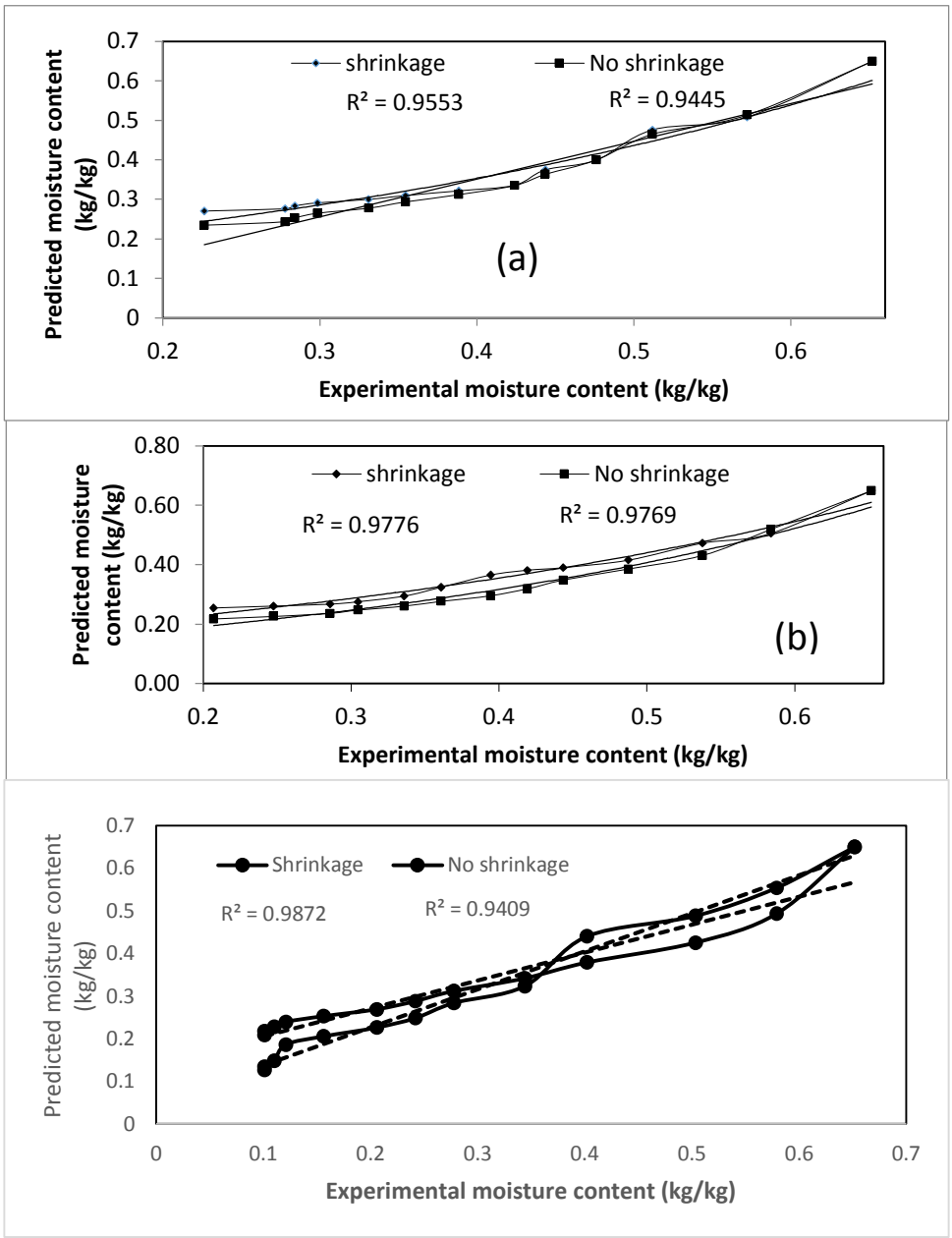

Fig. 5: Predicted and experimental moisture gradient (a) 60 °C (b) 70 °C (c) 80 °C.

3.3 Shrinkage based effective moisture diffusivity

The average effective moisture diffusivity is presented in Table 3. Shrinkage based effective moisture diffusivity is lower than the no-shrinkage effective moisture diffusivity which shows the need to consider shrinkage in the diffusivity models. This observation has also been made by Reyes et al.[32]. The effective moisture diffusivity increased with temperature due to higher heat transfer potential at a higher temperature, resulting in increased moisture loss from the product [29]. Though no research has been carried out on the drying of spent grain cake, the obtained effective moisture diffusivity is lower than $0.68 - 2.15 \times 10^{7}$ m/s^2 given for olive Pomace with a similar sample thickness of 41 to 63 mm and temperature range of 50 to 80 ºC [33]. However, it is higher than that of olive pulp which varied from 3.13 to 8.52 x 10^{-10} m/s^2[29]. Generally, the effective moisture diffusivities increased with the decrease in moisture content (Figure 6). This might be a result of the complex moisture diffusion mechanism in biomaterials. Initially, liquid diffusion of moisture predominates and drives the moisture transfer process but as the material gains heat and becomes more porous moisture transfer is dominated by vapour diffusion, thus the moisture diffusivity increases.

Table 3:Average effective moisture diffusivity

Drying Temperature	60°C	70°C	80°C
Shrinkage	3.25175E-09	3.5498E-09	7.06794E-09
Non-Shrinkage	2.59278E-09	2.83043E-09	5.63562E-09

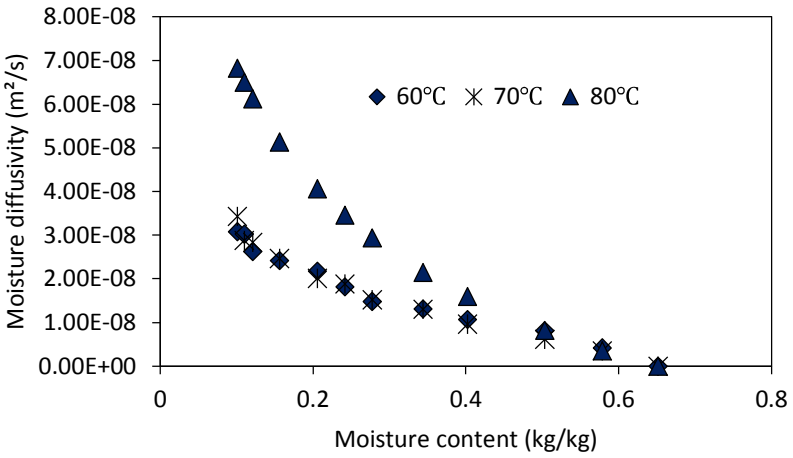

Fig.6.Effective moisture diffusivity variation with moisture content

This can be explained that the initial heat transfer potential to the product is low, resulting in lower energy of the internal moisture. Therefore, moisture transfer movement is lower due to the lower temperature of the moisture. However, as the drying progresses and the temperature of the moisture increases, the moisture content decreases, and the internal moisture gains more energy which increases the speed of moisture movement through the pores through the capillaries to the surface for moisture transfer to occur. Therefore, the effective moisture diffusivity increases. Similar results have been reported for mint, amioca and bamboo shoot slices [34, 35]. The combined influence of drying time (t) and temperature (T) on shrinkage effective moisture diffusivity is given by a power function equation expressed as follows

$$D_{eff} = 2.256 \times 10^{-9} \times t^{0.9375} \times T^{0.2676} \quad (R^2 = 0.99) \qquad 40$$

Where 2.256 x10^{-9} corresponds to the reference moisture diffusivity. However, the influence of moisture content (X) and the drying temperature on the effective moisture diffusivity is given in Equation. 41 as follows

$$D_{eff} = -3.6 \times 10^{-9} - 3.72 \times 10^{-8} \times ln(X) - 3.225 \times 10^{-9} \times ln(T) \quad (R^2 = 0.99) \qquad 41$$

The combined effect of moisture content, temperature and drying time was also empirically fitted with the linear equation as follows

$$D_{eff} = 6.695 \times 10^{-8} - 1.296 \times 10^{-7}(X) - 1.055 \times 10^{-10}(T) - 9.99 \times 10^{-10}(t) \quad (R^2 = 0.96) \quad 42$$

The no-shrinkage activation energy was deduced by the methods of slopes [36] as shown in Figure 7. The obtained value for cereal pulp is 37.63 kJ/mol while the diffusivity coefficient was deduced as 0.0.014 m^2/s. These values are within the range obtained in the literature [36].

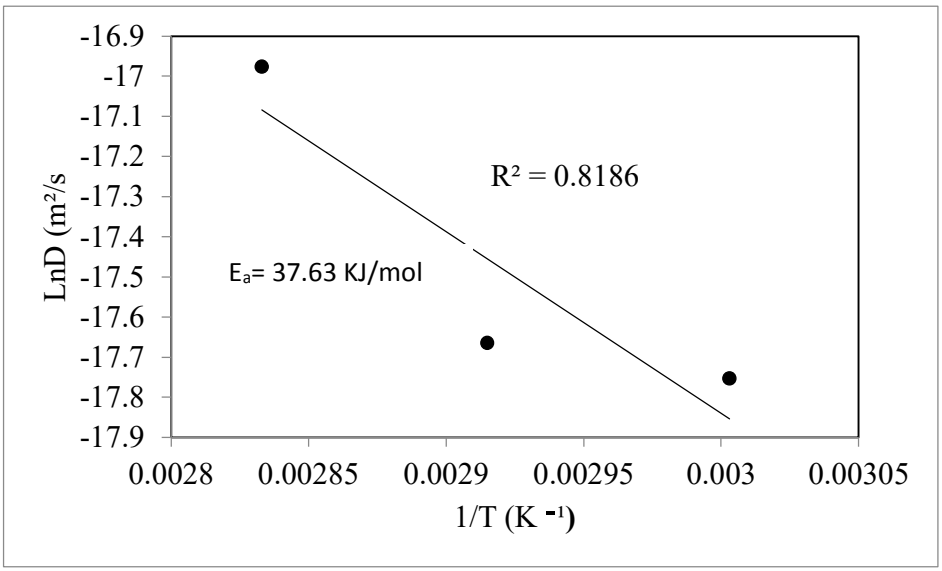

Fig.7. The plot of the Arrhenius relationship for effective moisture diffusivity (De) with drying temperature (T)

3.4 Mathematical modelling of drying curve

Table 4 presents the modelling parameters of the selected three thin layer diffusion models for the pellets. The three models performed well with R^2 and SE values of 0.98- 0.99, 0.0176 - 0.0259 and respectively. The drying constants (k) were high due to high drying rates for the pellets. However, looking at R^2 and SE values of the three selected models showed that the logarithmic model was best to describe the experimental data for drying at 60 and 70 °C while Henderson and Pabis gave a better result for drying at 80°C. Figure8 (a-c) showed the comparison of the best-fitted models with the experimental moisture ratios for varying time and temperatures. All the drying temperatures showed a good trend between the experimental and predicted data like the products dry as shown in Figure 9. The obtained coefficient of determinations is in the range of 0.99 for the three drying temperatures used. This showed that the Logarithmic models and Henderson and Pabis model can be used to predict the moisture ratio of the pellets under the variable condition used for the experiment.

Table 4: Result of fitting the selected drying models at different drying temperatures

Model	Oven drying method		
	60 °C	70 °C	80 ° C
Page			
K	0.1741	0.1750	0.3325
R^2	0.9899	0.9960	0.9961
SE	0.0239	0.0183	0.0259
Henderson and Pabis			
A	0.9593	0.9984	1.0350
K	0.1617	0.1703	0.3457
R^2	0.9945	0.9966	0.9978
SE	0.0211	0.0176	0.0227
Logarithmic			
A	0.8184	1.0684	1.0594
C	0.1543	-0.0898	-0.0303
K	0.2160	0.1488	0.3245
R^2	0.9954	0.9967	0.9974
SE	0.0203	0.0181	0.0232

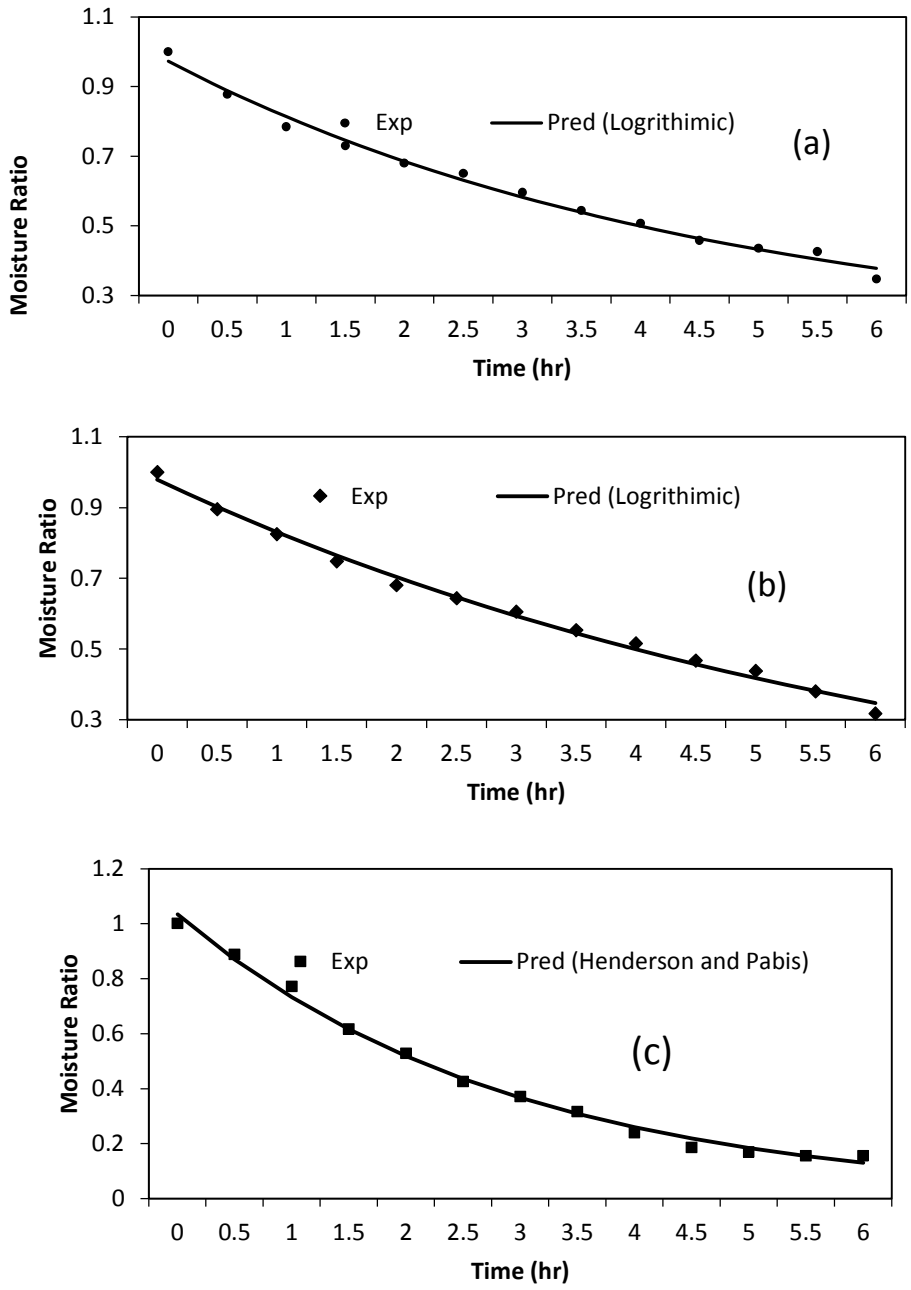

Fig.8. Experiment and Predicted moisture for different dying treatments (a) 60 ºC (b) 70 ºC (c) 80ºC

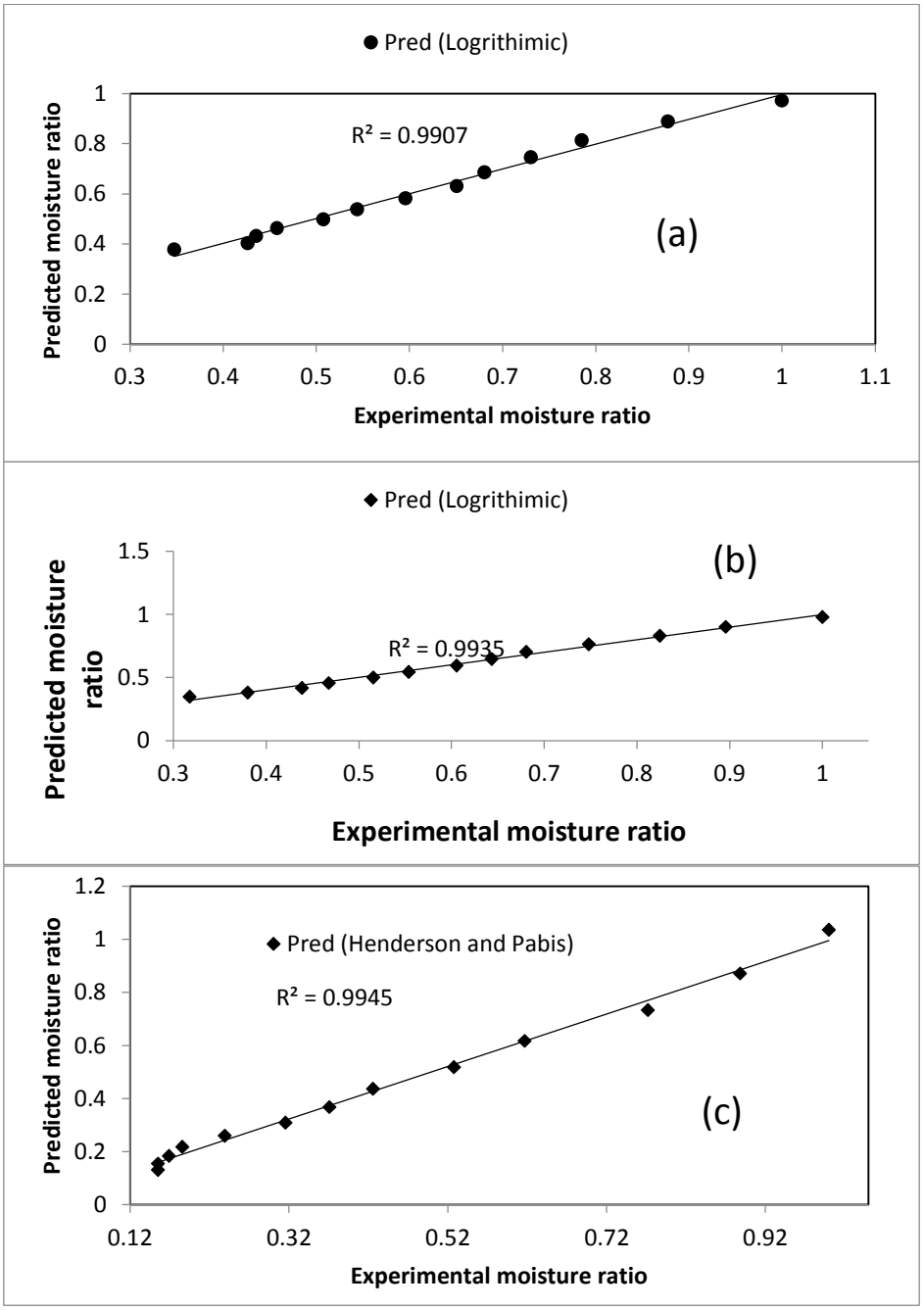

Fig. 9. predicted and experimental moisture ratio (a) 60 ºC (b) 70 ºC (c) 80 ºC.

3.5 Thermo-physical properties

Table 5 shows the average values of the specific heat capacity and thermal conductivity of the pellets at different temperatures. The two thermal properties decreased with an increase in drying temperature. Figures 10 and 11 indicated that moisture loss is associated with a decrease in specific heat and thermal conductivity. Loss of moisture is associated with loss of nutrients and these two parameters have a linear relationship with the specific heat capacity [25]. Higher temperature quickens the loss of moisture content by increasing the drying rate and at the same time

enhances the loss of volatile constituents which escape with the moisture content loss. When this happens, voids are created, leading to an increase in the diffusion path of the water molecules [37]. Therefore the heat transfer coefficient of the material decreases with the thermal conductivity [38]. This shows that moisture content is the key factor that influences the heat distribution during the drying of the pellets. This has also been reported by other researchers for agricultural materials [39,40]. The specific heat capacity ranges from 2767.67 to 9827.408 J/kg/°K for 60 °C, 2491.745 to 9827.408 J/kg/°K for 70 °C and 2302.769 to 9827.408 J/kg/°K for 80 °C as the moisture contents ranges from 12 51 ± 2.5 % to 65.18%. The average values for this range of values were shown in Table 5 for the three temperatures used. In contrast, the thermal conductivity ranges 0.11392 to 0.117124 W/m °K for 60 °C, 0.124953 to 0.128268 W/m °K for 70 °C and 0.135392 to 0.138985 W/m °K for 80 °C. The specific heat capacity of the spent grain is very high compared to maize grain (3404.8 – 3224.7 J/kg/°K), millet grain (3586.9 – 3224.7 J/kg/°K), or sorghum grain (3046.5 – 3224.7 J/kg/°K) at a moisture range of 5- 25.4 % due to very high initial moisture content [41, 42]. However, they approached the same values as the spent grain dries to equilibrium moisture content.

Table 5: Average values of the thermo-physical properties of spent grain pellets

Properties	Oven drying method		
	60°C	70 °C	80 ° C
Specific heat capacity(J/kgK)	5198.197	5691.993	5423.387
Thermal conductivity (W/m.K)	0.115281	0.126397	0.136882

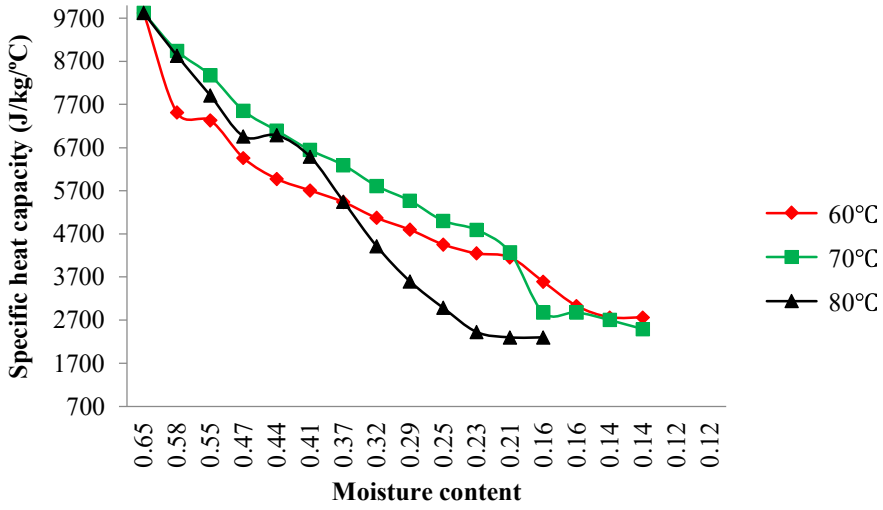

Fig. 10. Variation of the specific heat capacity with moisture content

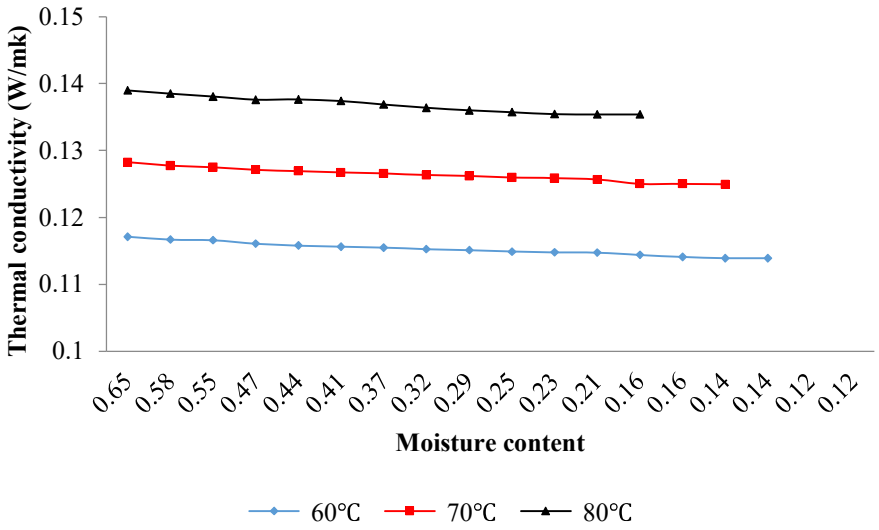

Fig. 11. Variation of the thermal conductivity with moisture content

3.6 Energy analysis of the drying process

The effect of drying temperature on the energy and specific energy consumption (SEC) are presented in Figures 12 and 13 respectively. Specific energy consumptions indicate the effectiveness of the energy utilization in the moisture removal process. It is a tool in energy management to identify improvement potential for energy efficiency. The lower the specific energy consumption for drying purposes, the better the energy utilization. The obtained results showed that the energy and specific energy consumption increased with temperature. The values ranged between 0.41 to 0.494 kWh and 108.39 to 119.29MJ/kg water respectively. From the specific energy consumption analysis, drying at a low temperature of 60°C is energy utilization effective compares to other temperatures. The relationships between the energy consumption, drying temperature and air velocity are given in equations 43 and 44 with R^2 values of 0.9994 and 0.9796 respectively. These showed a high degree of association between the energy consumption and the two drying parameters of air velocity and temperature. The result obtained is similar to that of Ndukwu et al [16] in fixed bed drying of piclirima Nitida seeds.

$$E_c = \frac{vT}{5377 - 6622v + 0.63T} \qquad R^2 = 0.9994 \qquad 43$$

$$E_{sp} = \frac{vT}{-3.364 - 11.05Ln(v) + 0.328Ln(T)} \qquad R^2 = 0.9796 \qquad 44$$

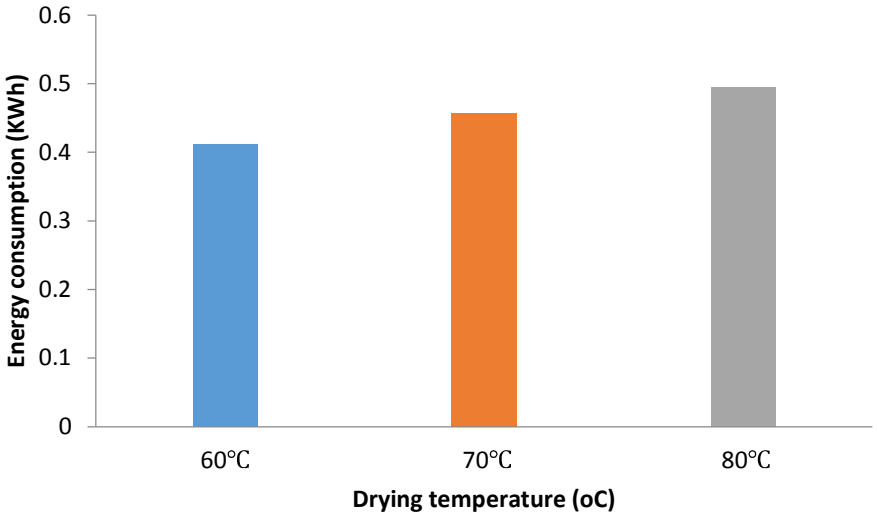

Figure 12. Effect of drying temperature on the energy consumption

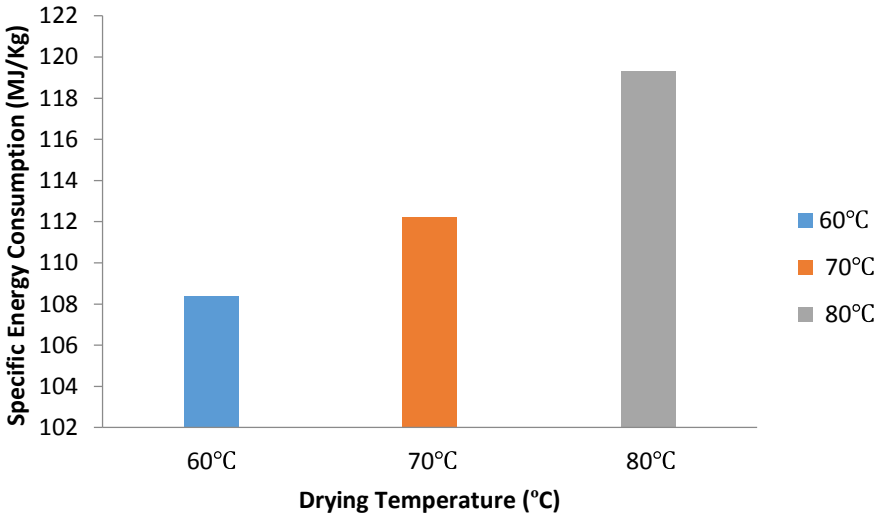

Figure 13. Effect of drying temperature on the specific energy consumption.

4. Conclusions

The influence of temperature and geometry deformation on the moisture evolution of spent grain pellets from pap production was studied. The modified Cranck's diffusion model was applied to predict the moisture loss behaviour with the introduction of shrinkage. The verification of the model showed a lower error value with the experimental moisture content when shrinkage was introduced. The effective moisture diffusivity with integrating shrinkage is lower than non- shrinkage though these values varied with drying time. The reliability of the developed model was verified using mean absolute error (MAE), and standard error (SE). The obtained values of MAE for moisture content with shrinkage were 0.0367 - 0.1500 and 0.0729 - 0.1500 for 60- 80 °C without shrinkage for the three temperatures used. The standard error values ranged from 0.019115 - 0.052146 for 60-80°C for shrinkage and 0.0267 - 0.0432 for without shrinkage. The relative error showed that integrating shrinkage under-predicted the

moisture values by 9.09 -19.83 % at 60-80 ºC. Additionally, it was 18.07-25.94 % without shrinkage. The lower values of these errors specify a better prediction capability of the model with the integration of shrinkage. Fitting the moisture ratio with the exponential drying curve equations shows that logarithmic equations were the best model for drying at 60 and 70 ºC while Henderson and Pabis's model was better at 80 ºC isothermal drying. Thermo-physical analysis showed that the average specific heat capacity ranges from 5423.387 to 5198.197J/kgK while the thermal conductivity ranged from 0.115281to 0.136882W/mK at 60-80 ºC. The energy and specific energy consumption ranged from 0.41 to 0.494 kWh and 108.39 to 119.29MJ/kg. The shrinkage ratios, effective diffusivity and energy and specific energy consumption were empirically presented as a function of moisture, temperature and or air velocity variations with a high degree of association. The data generated will help develop a fixed bed dryer to process spent grains to fuel at a lower scale to augment the energy needs of homes. As a perspective for the present work, the integration of solar energy sources to dry spent grain pellets could present an advantageous solution to reduce energy costs [46]. The use of solar air heaters for hot dry air production, its effect on the spent grain pellets drying process, its environmental impact and its economic feasibility will be presented in future works. Additionally, we will process the pellets to generate bio-oil and biochar using pyrolysis methods [43, 44].

Acknowledgements
We would like to express my appreciation to Dr Klein Ileleji, Professor of Agricultural & Biological Engineering at Purdue University for his help in reviewing this manuscript before its submission to the journal for review

Declarations
- The authors have no relevant financial or non-financial interests to disclose.
- The authors have no conflicts of interest to declare that they are relevant to the content of this article.
- All authors certify that they have no affiliations with or involvement in any organization or entity with any financial or non-financial interest in the subject matter or materials discussed in this manuscript.
- The authors have no financial or proprietary interests in any material discussed in this article.

Funding
This research received no funding or support from any organization

Conflicts of interest/Competing interests
There is no conflict of interest whatsoever among the authors or institutions

Availability of data and material
Not applicable

Code availability
Not applicable

References

1. Oniofiok N, D.O.Nnanyeleugo (1998). Weaning food in west Africa: nutritional problems and possible solutions.medicine, food and nutrition bulletin. Doi:10.1177/156482659801900105.
2. George-Okafor U.O. and Anosike, E.E. (2011).Fermented Corn Waste Liquor as a Potential Source for Probiotic Lactic Acid Bacteria. Nig J. Biotech. Vol. 22 (2011) 17- 22
3. McClurkin J D., K E.Ileleji (2015). The effect of storage temperature and percentage of condensed distillers solubles on the shelf-life of distiller's wet grains stored aerobically. Journal of Stored Products Research 62 (2015) 58-64
4. Cleveland, T.E., Dowd, P.F., Desjardins, A.E., Bhatnagar, D., Cotty, P.J., 2003. United States department of agriculture e agricultural research on pre-harvest prevention of mycotoxins and mycotoxigenic fungi in U.S. crops. Pest Manag. Sci. 59, 629-642.

5. FDA 1994.Office of Regulatory Affairs (ORA) Compliance Policy Guides (CPG) 7126.33 Sec. 683.100 - Action Levels for Aflatoxin in Animal Feeds
6. FDA Compliance Policy 7126.33: Section 683.100, November 21, 1979. Action Levels for Aflatoxins in Animal Feeds revised August 28, 1994.
7. US Department of Agriculture (USDA) Grain Inspection, Packers and Stockyards Administration (GIPSA) Backgrounder - Deoxynivalenol (DON), November 2001. (www.usda.gov/gipsa).
8. Torrecilla, J.S.; Aragon, J.M.; Palancar, M.C. Improvement of fluidized-bed dryers for drying solid waste (olive pomace) in olive oil mills. European Journal of Lipid Science and Technology 2006,108, 913–924.
9. Bennamoun L (2013). Improving Solar Dryers' Performances Using Design and Thermal Heat Storage. Food Eng Rev 2013; 5:230–248.
10. Milczarek, R.R.; Dai, A.A.; Otoni, C.G.; McHugh, T.H. Effect of shrinkage on isothermal drying behaviour of 2-phase olive mill waste.Journal of Food Engineering 2011, 103, 434–441.
11. San José M. J., S. Alvarez & R. López (2018): Drying of industrial sludge waste in a conical spouted bed dryer. Effect of air temperature and air velocity, Drying Technology, DOI: 10.1080/07373937.2018.1441155
12. Onwude D.I., Hashim, N., Abdan, K., Janius, R., Chen, G., Kumar, C., Modeling of coupled heat and mass transfer for combined infrared and hot-air drying of sweet potato. J. Food Eng. 228 (2018) 12–24. doi:10.1016/j.jfoodeng.2018.02.006
13. Bennamoun L, R Khamab,c, A Léonard (2015). Convective drying of a single cherry tomato: Modeling and experimental study. Food and bioproducts processing 9 4, 114–123. http://dx.doi.org/10.1016/j.fbp.2015.02.006
14. Efremov G. and T. Kudra (2005). Model-Based Estimate for Time-Dependent Apparent Diffusivity. Drying Technology, 23: 2513–2522, 2005
15. Kaleemullah S, R. Kailappan (2004). Moisture sorption isotherms of red chillies. Biosystems Engineering 88 (1) 95–104.
16. Ndukwu M. C., L. Bennamoun, O. Anozie Evolution of thermo-physical properties of Akuama (picralima nitida) seed and antioxidants retention capacity during hot air drying. Heat Mass Transfer (2018) 54:3533-3546,DOI 10.1007/s00231-018-2379-2
17. Simo-Tagne M, H D Tamkam Etala, A Tagne Tagne, M C Ndukwu, M El Marouani (2022)Energy, environmental and economic analyses of an indirect cocoa bean solar dryer: A comparison between natural and forced convection. Renewable Energy 187 (2022) 1154-1172
18. Vaibhav, T., Anil1, D. S., and Pradeep, P. P. (2018). Investigation of Heat Transfer Coefficient in 'Square Shaped Pin-Fin'. International Journal of Advanced Research in Science and Engineering (IJARSE), 7(3), 2319 – 8354.
19. Simo-Tagne, M.; Ndukwu, M.C.; Zoulalian, A.; Bennamoun, L.;Kifani-Sahban, F.; Rogaume, Y. (2020). Numerical analysis and validation of a natural convection mix-mode solar dryer for drying red chilli under variable conditions. *Renewable Energy.* 2020, 151, 659-673.
20. Simo-Tagne M., M.C. Ndukwu, Study on the effect of conical and parabolic solar concentrator designs on hybrid solar dryers for apricots under variable conditions: a numerical simulation approach, Int. J. Green Energy (2021), https://doi.org/10.1080/15435075.2021.1914632.
21. Das Purkayastha, M., Nath, A., Deka, B.C. *et a (2013).* Thin layer drying of tomato slices. *J Food Sci Technol* **50,** 642–653
22. Kumar, C., Millar, G.J., Karim, M. a, 2014b. Effective diffusivity and evaporative cooling in convective drying of food material. Dry. Technol. 33, 227-237.https://doi.org/10.1080/07373937.2014.947512
23. Ariku A.Y., N.A. Aviara, S.C. Ahamefule, U.C. Abada, N. Eke-emeziee, M. Simo-Tagne (2012). Specific heat capacity of selected legumes and cereals grain grown in North-Eastern Nigeria. Arid Zone journal of engineering, technology and environment, 8, 105-114
24. Motevali A, Minaee S (2011) Evaluation of energy consumption in different drying methods. Energy Convers Manag 52:1192–1199

25. Ihediwa V.E., M.C. Ndukwu, U.C. Abada, E. Inemesit-Ekop, L. Bennamoun, M. Simo-Tagne, F.I. Abam, Optimization of the energy consumption, drying kinetics and evolution of thermo-physical properties of drying of forage grass for haymaking, Heat Mass Tran. (2021), https://doi.org/10.1007/s00231-021-03146-2.

26. Baniasadi E., S. Ranjbar, O. Boostanipour, Experimental investigation of the performance of a mixed-mode solar dryer with thermal energy storage, Renew. Energy 2017 (2017), https://doi.org/10.1016/j.renene.2017.05.043

27. Hamdaoui Ali M., M. Hichem Benzaama, Y. El Mendili, D. Chateigner, A review on physical and data-driven modelling of buildings hygrothermal behaviour: models, approaches and simulation tools, *Energy & Buildings* (2021), DOI: https://doi.org/10.1016/j.enbuild.2021.111343

28. Baeh H. D. r and K. Stephan, "Mass transfer Theory," in *Heat and Mass Transfer*, Berlin, Heidelberg: Springer Berlin Heidelberg, 2011, pp. 87–102. doi: 10.1007/978-3-642-20021-2.

29. Goula A M., Athanasios N. Chasekioglou& Harris N. Lazarides (2015): Drying and Shrinkage Kinetics of Solid Waste of Olive Oil Processing, Drying Technology: An International Journal, DOI: 10.1080/07373937.2015.1026983

30. Szentmarjay, T.; Pallai, E.; Regenyi, Z. Short-time drying of heat-sensitive, biologically active pulps and pastes. Drying Technology 1996, 14(9), 2091–2115.

31. Jumah, R.; Al-Kteimat, E.; Al-Hamad, A.; Telfah, E. Constant and intermittent drying characteristics of the olive cake. Drying Technology 2007, 25, 1421–1426

32. Reyes A., J. Vásquez, N. Pailahueque& A. Mahn (2018): Effect of drying using solar energy and phase change material on kiwifruit properties, Drying Technology, DOI: 10.1080/07373937.2018.1450268

33. Meziane, S. Drying kinetics of olive pomace in a fluidized bed dryer.Energy Conversion and Management 2011, 52, 1644–1649.

34. Karathanos, V. T., Kanellopoulos, N. K., and Belessiotis, V.G. (1996). Development of porous structure during air drying of agricultural plant products. Journal of Food Engineering. 29: 167-183.

35. Ozbek, B.; Dadali, G. Thin-layer drying characteristics and modelling of mint leaves undergoing microwave treatment. Journal of Food Engineering 2007, 83(4), 541–549.

36. Ndukwu M.C., A.S Ogunlowo, O.J. Olukunle. Cocoa Bean (Theobroma cacao L) drying kinetics. Chilean J. Appl. Agric. 70 (4) (2010) 633-639

37. Ndukwu MC, Bennamoun L, Anozie O (2018) Evolution of thermo-physical properties of Akuama (picralima nitida) seed and antioxidants retention capacity during hot air drying. Heat and Mass Transf 54:3533–3546

38. Khalloufi S, Almeida-Rivera C, Janssen J, Bongers P (2012) Pseudo-linearity of the shrinkage coefficient and a sensitivity study of collapse and shrinkage functions. Food Res Int 48:808–819

39. Martynenko AI (2011) Porosity evaluation of ginseng roots from real-time imaging and mass measurements. Food Bioprocess Technol 4:417–428

40. Madiouli J, Sghaier J, Lecomte D, Sammouda H (2012)Determination of porosity change from shrinkage curves during drying of food material. Food Bioprod Process 90:43–51

41. Chen XD, Xie GZ, Rahman MS (1998) Application of the distribution factor concept in correlating thermal conductivity data for fruits and vegetables. Int J Food Prop 1(1):35–44

42. Turgut A, Tavman I (2009) And Tavman, S. Measurement of thermal conductivity of edible oils using transient hot-wire method. Int JFood Prop 12:741–747

43. Horsfall I.T, M. C. Ndukwu, · F. Abam, M. Simo-Tagne, C. C Nwachukwu. (2022). Parametric studies of heat and mass transfer process for two-stage biochar production from poultry litter pellet biomass. Biomass Conversion and Biorefinery https://doi.org/10.1007/s13399-022-02774-w

44. M.C. Ndukwu and I.T. Horsfall (2020).Prospects of Pyrolysis Process and Models in Bioenergy Generation: a Comprehensive Review. Polytechnica (2020) 3:43–53

45. Dutta S. K.; V. K. Nema; R. K. Bhardwaj (1988). Thermal Properties of Gram J agric. Engng Res., 39, 269-275

46. Simo-Tagne M , H D Tamkam Etala , Ab Tagne-Tagne , M C Ndukwu, M El Marouani (2022).Energy, environmental and economic analyses of an indirect cocoa bean solar dryer: A comparison between natural and forced convection . Renewable energy, 187, 1154 - 1172